Talanta 260 (2023) 124605

Contents lists available at ScienceDirect

Talanta

journal homepage: www.elsevier.com/locate/talanta

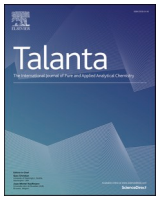

A non-destructive X-ray fluorescence method of analysis of formalin fixed-paraffin embedded biopsied samples for biomarkers for breast and colon cancer

Sofia Pessanha [a,b,*], Daniel Braga [a], Ana Ensina [a], João Silva [a], José Vilchez [c], Carlos Montenegro [c], Sofia Barbosa [a,d], Maria Luísa Carvalho [a,b], António Dias [a,b]

[a] NOVA School of Sciences and Technology, Campus Caparica, 2829-516, Caparica, Portugal
[b] Laboratory of Instrumentation, Biomedical Engineering and Radiation Physics, Campus Caparica, 2829-516, Caparica, Portugal
[c] Centro Hospitalar Barreiro- Montijo, Av. Movimento das Forças Armadas 79C, 2830-003, Barreiro, Portugal
[d] GeoBioTec, Campus Caparica, 2829-516, Caparica, Portugal

ARTICLE INFO

Keywords:
Cancer
Formalin-fixed paraffin-embedded
Biological tissues
Biomarkers
EDXRF

ABSTRACT

In this work we present a methodology for the non-destructive elemental determination of formalin-fixed paraffin-embedded (*FFPE)* human tissue samples based on the Fundamental Parameters method for the quantification of micro Energy Dispersive X Ray Fluorescence (micro-EDXRF) area scans.

This methodology intended to overcome two major constraints in the analysis of paraffin embedded tissue samples – retrieval of optimal region of analysis of the tissue within the paraffin block and the determination of the dark matrix composition of the biopsied sample. This way, an image treatment algorithm, based on R® tool to select the regions of the micro-EDXRF area scans was developed. Also, different dark matrix compositions were evaluated using varying combinations of H, C, N and O until the most accurate matrix was found: 8% H, 15% C, 1% N and 60% O for breast FFPE samples and 8% H, 23% C, 2% N and 55% O for colon. The developed methodology was applied to paired normal-tumour samples of breast and colon biopsied tissues in order to gauge potential elemental biomarkers for carcinogenesis in these tissues. The obtained results showed distinctive biomarkers for breast and for colon: there was a significant increase of P, S, K and Fe in both tissues, while a significant increase of Ca an Zn concentrations was also determined for breast tumour samples.

1. Introduction

Current diagnostic and therapeutic approach for cancer is based on well-established predictive and prognostic factors. Some have been broadly studied, others lack validation in statistically robust studies. Considering the worldwide increasing prevalence of cancer and the possible contribution of trace elements to carcinogenesis reported in some studies [1,2], it is pertinent to analyse trace element content in normal and cancerous tissues: over 96% of the weight of the average human body is composed of four main elements (H, O, C and N), while the remaining is made up of minor (Na, K, Mg, Ca, Cl, P, S) and trace (Mn, Fe, Cu, Zn, Se) elements [3,4]. These elements play important roles in biological processes and association between them and the presence of diseases has already been uncovered [1]. For instance, Ca is involved in many cellular processes, namely, apoptosis and angiogenesis [3], while Cu and Zn are cofactors or essential components of nearly 300 enzymes. Fe is present at the active site of many molecules that are instrumental in biological functions such as oxygen transport, electron transfer, and DNA synthesis [2], while Se is required as an essential cofactor for antioxidant enzymes, such as glutathione peroxidases [4].

Accurate evaluation of trace elements in tissues allows for the establishment of possible correlations between the various elements and factors like age, sex, and stage of disease, leading to a better understanding of carcinogenesis. Energy Dispersive X-ray Fluorescence (EDXRF) is a spectroscopic technique that already made inroads in the analysis of human tissues [5–11]. Magalhães et al. analysed normal and carcinoma tissues with EDXRF and reported increased or constant levels of Fe and Cu and decreased levels of Zn [8]. For this study, samples were

Abbreviations: FFPE, Formalin Fixed Paraffin Embedded.

* Corresponding author. NOVA School of Sciences and Technology, Campus Caparica, 2829-516, Caparica, Portugal.
E-mail address: sofia.pessanha@fct.unl.pt (S. Pessanha).

https://doi.org/10.1016/j.talanta.2023.124605
Received 4 March 2023; Received in revised form 28 March 2023; Accepted 25 April 2023
Available online 29 April 2023

freeze-dried, powdered, and pelletized and the FP-method was applied for quantification. This method estimates a composition for the unknown sample by calculating the theoretical fluorescence intensities and iteratively comparing them with the measured ones, until the best correspondence between calculated and experimental spectra is obtained [12]. The accuracy of these determinations relies on many factors, namely, the knowledge of the spectral distribution of the excitation radiation [13] and the estimation of the matrix composition [11]. This can be difficult to achieve when applying polychromatic excitation using focusing optics in the study of samples such as human soft tissues, with an unknown dark matrix.

Accurate quantitative determinations in EDXRF requires the use of suitable empirical and/or mathematical methods for the conversion of the fluorescent intensities of the spectra into the concentration of the element in the sample [14]. This approach was used for the determination of the concentrations of Mn, Fe, Cu, and Zn and their correlations with the clinical stage of the prostate cancer, using two homemade standards, prepared using N,N′-methylenebisacrylamide mixed with different aqueous solutions of metal nitrates [15,16].

This approach was also used to study the K, Ca, Mn, Fe, Cu and Zn concentrations in breast tissues by means of calibration curves constructed with reference water solutions of known concentrations in order to simulate the matrix effects of healthy tissues as well as of neoplastic ones [10,17,18]. The methodology was further improved by Silva et al. [5] that used the scattered radiation in each XRF spectrum to correct the calibration curve and improve accuracy of the quantification of normal and neoplastic breast tissue.

However, there is always a great impairment to statistically significant conclusions of the implemented investigations: the extremely reduced number of samples. Additionally, the corresponding normal tissue is seldom available for comparison and exclusion of biological variability.

In order to overcome this obstacle, it could be useful to take advantage of the vast repository of human tissue samples, fixed in formalin and embedded in paraffin, that are stored in hospitals after biopsies and surgeries. The analysis of these tissues could allow drawing significant conclusions about the characterization and comparison of normal and tumour tissues for different organ types, as well as establishing correlations between elemental concentration and other factors such as age, gender, and disease stage.

The analysis of these *FFPE* samples has been performed previously for the evaluation of the differential impact of time storage on the quality, quantity, and degradation of viral and human DNA employing a quantitative PCR on *FFPE* invasive cervical cancer samples HPV16 single infected that had been archived for 15 and 85 years [19], proving how valuable and sometimes disregarded sources of information these samples are.

The analysis of *FFPE* tissues has also been attempted previously using atomic spectrometry techniques, but always in a destructive manner: slicing the paraffin block into a thin film [20,21], digesting the sample for the analysis of the solution [22], or analysis after de-paraffinization [23] Such methodologies would be unacceptable for the analysis of tumour tissue samples stored in paraffin blocks, as future investigations with benefit for the patients (e.g., identification of biomarkers for the use of novel drugs) or their families (e.g., identification of hereditable parameters/biomarkers of risk) would be impaired.

However, there is a major disadvantage when using these samples, namely the substrate, that increases the factor of greatest uncertainty in the quantification by EDXRF: the characterization of the dark matrix of the sample. The dark matrix is composed of the four main elements present in biological matrices, H, C, O and N, elements that are not visible in an EDXRF spectrum, but significantly influence how the remaining elements of interest are detected.

In this work we present a methodology for the quantification of the elements present in formalin-fixed paraffin-embedded human tissue samples using Fundamental-Parameter method. The dark matrix composition was assessed through the evaluation of the mean-Z of the sample using a calibration curve based on the determination of the Compton-to-Rayleigh ratio in the EDXRF spectrum [24].

This quantitative model will ultimately be applied to FFPE tissues from colon and breast tissues in order to compare the elemental content of tumour and normal tissues extracted from the surgical margins, in order to gauge possible biomarkers for cancer. The main advantage of this new method is to benefit from the information of the FFPE samples in storage in medical facilities in a fully non-destructive approach.

2. Experimental design

The paraffin-embedding poses as a hindrance in accurate quantification in EDXRF. Besides changing the dark matrix of the sample, a layer of unknown thickness of paraffin (C_nH_{2n+2}) over the tissue must also be taken into account.

In order to select the region of the sample, the following methodology (Fig. 1) was undertaken:

1) Perform area measurements of the samples using scanning μ-EDXRF;
2) Inspect the elemental map of Sulphur (S Ka = 2.3 keV) - the rationale behind choosing this element was threefold:
   - It's low emission energy is sensitive to attenuation in paraffin;
   - It is present in high amounts in human tissue (within thousands of $\mu g.g^{-1}$) in an homogeneous fashion;
   - It is not present in paraffin, even as an impurity;
3) Use an image treatment algorithm, based on R® tool to select the areas with higher Sulphur signal;
4) Extract the EDXRF spectrum corresponding to the selected area using the MSprit® tool.

2.1. Micro-EDXRF experimental setup

The μ-EDXRF system used was the M4 Tornado (Bruker, Germany). The X-ray tube is a micro-focus side window low-power Rh tube, operated at 50 kV and 300 μA. A polycapillary lens was used to obtain a spot size down to 25 μm for Mo-Kα. Detection of fluorescence radiation was performed by a silicon drift detector with 30 mm^2 sensitive area and energy resolution of 142 eV for Mn-Kα. To ensure representative evaluation of the composition, instead of spot analysis, area acquisition was performed and the accumulated spectrum was evaluated. Mappings were performed encompassing the whole sample area using a step size of 25 μm and time per step of 12 ms/pixel. Two scans were obtained with different filter configurations (between X Ray tube and sample) using a 12.5 μm Al filter to remove the L-series scattering lines of Rh, and a multi-layered filter composed of 100 μm Al, 50 μm Ti and 25 μm Cu for background reduction and improvement of detection limits for higher Z elements ($Z \geq 20$).

2.2. Image analysis – R® tool

R is a free programming language software best suited for statistical data analysis and graphics [25]. One of R's main advantages is its easy extensibility through the use of packages, which broadens its potential applications beyond just the field of statistics. In order to select the best region for spectrum collection from the elemental map image file, two packages were used: R©Colordistance and R©Countcolors. By combining these two libraries, it is possible to select areas of images based on their colour or intensity. Using the R©Colordistance, a subset of 10000 randomly selected pixels from the S mapping image was selected in order to speed up the computing process. Each of those pixels was treated as a point in a three dimensional space according to their Red (R) Green (G) and Blue (B) values. Each of these axes ranges from 0 to 1, so pure red, for example, would have a red value of 1, a green value of 0, and a blue value of 0. Magenta, which is an equal mix of red

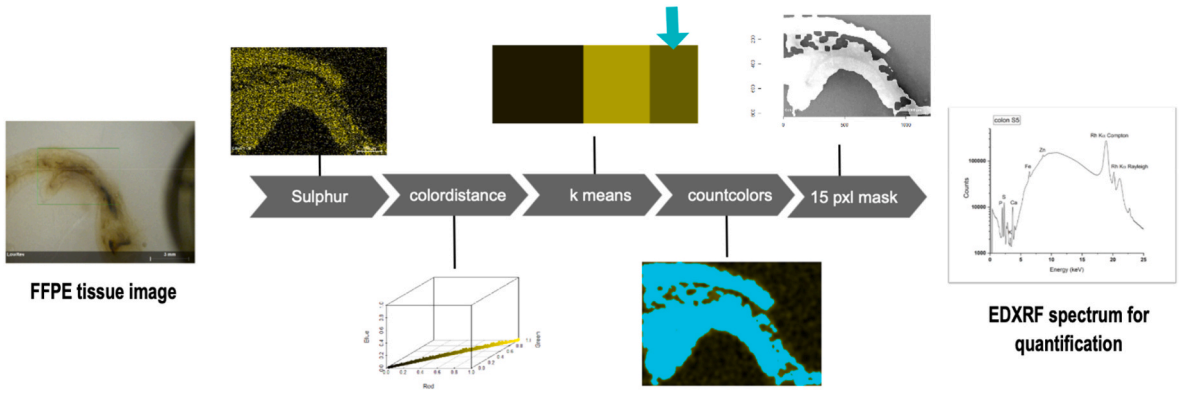

Fig. 1. Depiction of the developed methodology, from the selection of the area in the sample, acquisition of 2D elemental map of sulphur, use of R©Colordistance and R©Countcolors for selection of region of interest and collected spectrum for quantification.

and blue, would have an RGB triplet of [0,1,1]. Then, through the use of a k-means algorithm, the pixels were split into three different clusters, and the mean RGB values of each of them were stored. Then, by using the R©Countcolors, all pixels with higher intensity (higher RGB values) than the mean of the second most intense cluster were selected. To eliminate small holes in the selected area, a closing operation was performed (dilation followed by an erosion). A square mask with a size of 15 pixels was used. The selected area was then plotted over a grayscale picture of the sample, to facilitate its selection on the Tornado software for spectra extraction.

2.3. Formalin fixed paraffin embedded (FFPE) samples

For this study, samples were kindly provided by the Pathologic Anatomy unit of the Centro Hospitalar Barreiro Montijo, Barreiro, Portugal, after approval from the ethics committee. The samples consisted of storage specimens of surgically removed tissue from individuals diagnosed with breast or colon tumours, fixed in formalin and embedded in paraffin for preservation. All samples were duly anonymized, hence, the need for consent was waived by the ethics committee.

These FFPE samples were grouped into pairs of normal and tumour tissue from each individual. A total of 30 colon pairs and 28 breast pairs of samples were analysed without the need for any sample preparation or reagent addition. Fig. 2 shows the image of a pair of FFPE blocks for normal and tumour colon. Afterwards, samples were returned undamaged to the Hospital, for storage. Visual examination under a stereomicroscope revealed no apparent damages caused by the irradiation with X-ray source and handling during measurements.

2.4. Statistical analysis

The normality of the distributions of each of the trace elements on each kind of tissue (normal and tumour) was tested with the Shapiro-Wilk Test. The results of this test showed that some elements were normally distributed and others were not. Since not all elements were normally distributed, non-parametric tests were used to test for differences in the normal and tumour tissue distributions.

The non-parametric Kruskal-Wallis Test was used: this test infers differences in distributions based on the difference in the medians of those distributions. The tests' null hypothesis states that both distributions are alike, and can only be rejected if the p-value is inferior to 0.05.

3. Quantification methodology

Quantification was performed using MQuant®, an in-built software of the M4 TORNADO system, was used. This software allows spectra deconvolution, peak fitting, and quantification using the Fundamental Parameters method [26], but requires the matrix composition to be given as input. This code has been used successfully in the quantification of bone [27] exoskeletons [28] and metal samples [29] where either the matrix was known and entered in the software or all the elements were visible in the EDXRF spectrum.

3.1. Dark matrix determination

The determination of the sample's dark matrix was accomplished by evaluating the samples' mean Z. The suitability of comparing the

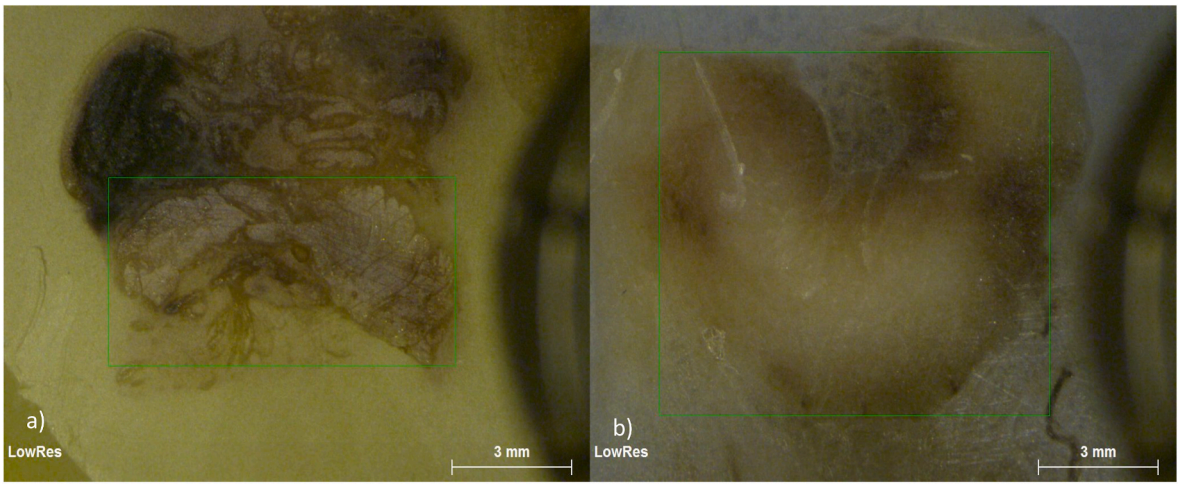

Fig. 2. Image of the FFPE tissue block taken with 10x camera inbuilt in the M4Tornado system a) normal tissue and b) tumour tissue.

Compton-to-Rayleigh ratio of the characteristic lines X Ray tube in an EDXRF spectrum to obtain the mean Z was already established [24,30]. For a given experimental configuration (scattering photon energy and geometry) a curve based on model samples of varying atomic number can be built, in order to gauge the dependence of the Compton-to-Rayleigh ratio with the sample's mean Z. In this work, such curve was built using model samples consisting of different proportions of reference materials of hydroxyapatite [$Ca_{10}(PO_4)_6(OH)_2$] (Sigma-Aldrich, lot #BCBS8492V), and boric acid [H_3BO_3] (for conservation purposes) [24], a 3 mm thick block of PMMA (polymethyl methacrylate) and a 10 mm thick block of paraffin (C_nH_{2n+2}, used for sample embedding). Fig. 3 shows the experimental curve obtained in this work and the results for the nonlinear curve fit undertaken.

In order to gauge the matrix average Z of the FFPE samples, the Compton-to-Rayleigh ratios of 8 samples from each tissue were determined. The mean Z was extrapolated to be 6.01 ± 0.05 for the colon samples, and 5.8 ± 0.1 for the breast samples. Figs. 4 and 5 present example spectra for breast sample S3 and colon sample S5, respectively.

It is noteworthy that the mean Z of the breast samples is smaller than the colon samples' mean Z. This was expected due to the higher adipose content of breast tissue. Moreover, the uncertainty in mean Z in breast is higher than for colon samples. This higher uncertainty in the breast samples' mean Z might be due to some variability introduced by different muscle/fat content within samples.

Considering the calculated mean Z values, a script was developed in R to compile multiple possible compositions of matrices. These compositions were chosen considering the available tissue compositions developed by the International Commission on Radiological Protection (ICRP) composition for soft tissue, for adipose tissue, for brain and lung tissue, the four component International Commission on Radiation Units and measurements (ICRU) composition for soft tissue [11] and considering an increase in C and H due to paraffin.

Out of the compiled compositions, the following, were selected for comparison (Table 1).

4. Results and discussion

4.1. Dark matrix determination

4.1.1. Dark matrix for formalin fixed paraffin embedded breast samples

The several Dark Matrices (DM) compositions for breast were essayed on the Formalin Fixed paraffin Embedded (FFPE) normal samples and the statistical differences between the results were evaluated. Fig. 6 displays, as example, the histograms of the quantitative determinations obtained for the elemental concentration of Ca and P. As can be seen, there is a great dispersion of the obtained values, as they

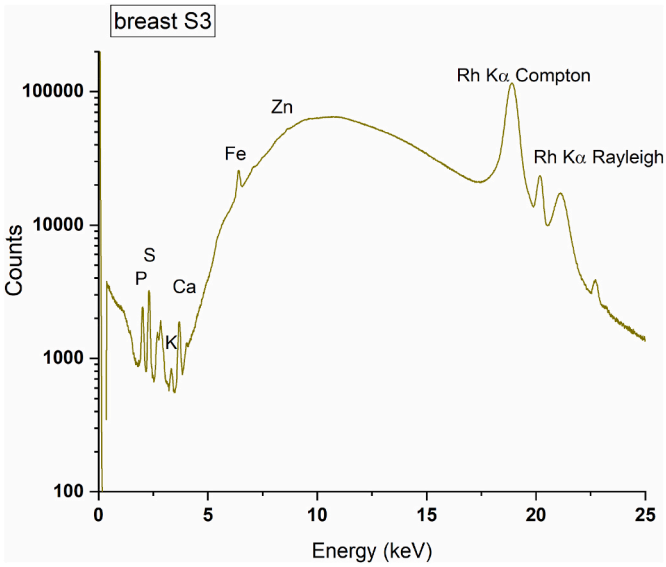

Fig. 4. Spectrum obtained for breast sample S3.

vary between sample, however, regardless of the used Dark Matrix, the distribution is very similar.

This was further evaluated using the Kruskal-Wallis ANOVA, for the comparison of the elemental quantifications of the 28 normal breast samples using the five essayed Dark Matrices. For all the tested elements, the populations were not significantly different ($p > 0.05$).

In order to evaluate the dispersion in quantification between matrices, the mean concentration for each element in each sample and deviation of each determination to the mean (%) was calculated. Table 2 presents the mean deviation (%) obtained with each Dark Matrix configuration. As can be seen, for all the analysed elements, the maximum deviation was 2%, while for some elements in some matrices there was no variation.

Considering the overall performance, and the fact that Ni was present in such low concentrations, the chosen matrix was DM_C presenting no variation values of 2%. Fig. 7 presents the boxplots for the elemental content of normal breast tissues using DM_C. The obtained values were compared with the quantitative determinations for this tissue (without formalin fixation and paraffin embedding) in literature using EDXRF but also other techniques such as Total Reflection X Ray Fluorescence (TXRF), Particle Induce X Ray Emission (PIXE) and Neutron Activation Analysis (NAA) (Table 3). As demonstrated by the determinations in Table 3, the obtained values for light elements (P, S, K and Ca) can vary

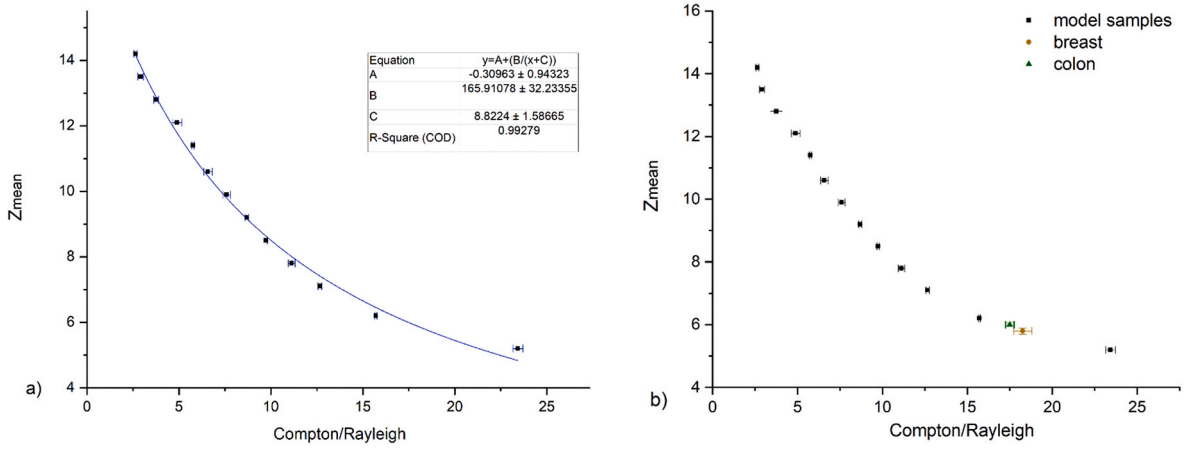

Fig. 3. Calibration curve for the dependency of mean atomic number and Compton-to-Rayleigh ratio in the used experimental setup a) for reference samples and b) including FFPE breast and colon tissues.

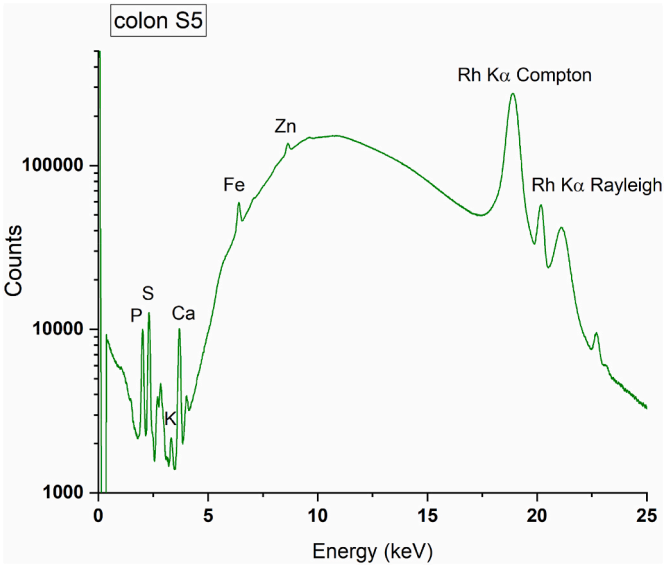

Fig. 5. Spectrum obtained for colon sample S5.

Table 1
Dark matrix compositions essayed for breast (DM_A to DM_E) and colon (DM_F to DM_J) samples. Compositions in % (w/w).

		H	C	N	O
breast	DM_A	8%	20%	2%	56%
	DM_B	8%	21%	2%	54%
	DM_C	8%	15%	1%	60%
	DM_D	10%	18%	1%	56%
	DM_E	5%	16%	1%	59%
colon	DM_F	11%	20%	3%	56%
	DM_G	13%	17%	3%	58%
	DM_H	8%	15%	2%	61%
	DM_I	8%	23%	2%	55%
	DM_J	5%	22%	1%	57%

from few hundreds of $\mu g.g^{-1}$ up to thousands of $\mu g.g^{-1}$, a behaviour also demonstrated by our method. The exception would be K, but our results comply with the determinations for normal breast tissue obtained by Magalhães et al. [31] using TXRF and a matrix independent method of quantification. Transition metals, Fe, Cu, Ni and Zn, are also present in a range of concentrations, with Fe and Zn reaching hundreds of $\mu g.g^{-1}$. Our results are also within the expected order of magnitude and range, with iron presenting high concentrations but similar to the concentrations determined by Garg et al. [32] using NAA.

4.1.2. Dark matrix for FFPE colon samples

The several DM compositions for colon were also tested on the FFPE normal tissue samples. Fig. 8 displays, as example, the boxplots obtained for the elemental concentration of S and Fe. As can be seen, the dispersion of the obtained values is also very similar regardless of the used Dark Matrix. Again, Kruskal-Wallis ANOVA test was used to compare the elemental quantifications of the 30 samples using the five essayed Dark Matrices. For all the tested elements, the populations were also not significantly different ($p > 0.05$).

Similarly to the methodology for breast, the mean concentration for each element in each sample obtained with the 5 dark matrices was determined and the mean variation to the mean, for each element is presented in Table 4.

As can be seen, for all the analysed elements, the maximum deviation was 5%, for matrix DM_F and 1% for matrix DM_I. This way, for further comparison of normal and tumour tissue, DM_I was chosen. The elemental concentration ranges for normal colon FFPE samples is presented in the boxplots of Fig. 9.

Regarding elemental quantification of colon samples, the literature is very scarce. However, comparing with the studies presented in Table 3, we can confirm that the obtained values for minor and trace elements are within the expected order of magnitude and in compliance with the elemental concentrations determined in colon tissue samples using destructive techniques that do not depend on the determination of the matrix. The main difference was obtained for K value, lower than the literature for colon, however, within the order of magnitude of concentration obtained for breast samples.

Considering this evaluation, the quantification method developed for FFPE breast and colon tissues was considered suitable and accurate for its application to the comparison of normal and tumour tissue. Moreover, the need for a different dark matrix for each type of sample under studied was highlighted by the resulting different compositions obtained.

4.2. Comparison of normal and tumour tissue

Fig. 10 displays the bar chart comparing the mean elemental concentration (± standard deviation) for 28 pairs of normal and tumour breast tissue.

The obtained results showed a very significant increase of P, S, Ca, Fe and Zn in the tumour tissue samples ($p < 0.001$) and a significant increase of K ($p < 0.05$) for the same tissues. Similar behaviour was determined by Poletti et al. [10] in the comparison of normal and tumour breast tissue from the same donor using Synchrotron radiation XRF and by Silva et al. [37] and Magalhães et al. [31] using TXRF. The difference would be in the determined increase of Cu in tumour tissue, unvaried in our samples. The increase of P, S, Ca and Fe was also determined by Badiger et al. [38] using similar methodology. Regarding Zn, the later only determined an increase of Zn in samples from middle age and senior donors (51–70 years old). Regarding Cu, the variation was also age-dependent – decrease for 41–50 years old group and increase for the remaining age groups. No age discrimination was performed in our study and by Poletti et al. [10], Silva et al. [37] and Magalhães et al. [31], so this can explain the discrepant results.

Breast cancer is the most common type of cancer in women worldwide. Perhaps for this reason, the study of elemental concentration regarding malignant breast tumour, has already been an area of proficient research.

Several studies have shown that available iron may promote malignancy, by playing an important role in cell growth regulation and by inducing oxidative stress, causing DNA, protein and organelle damage, through production of hydroxyl radicals and hydrogen peroxide via Haber–Weiss and Fenton-type reactions [36,39]. Zinc is a transition metal which is vital for the functioning of numerous cellular processes, is critical for growth, and may play an important role in cancer aetiology, namely breast cancer [40]. Work by Dutta et al. [41] suggests that cancer cells develop mechanisms to shut down zinc efflux and maintain intracellular concentrations when availability is reduced, demonstrating the importance of intracellular zinc for rapidly dividing cancer cells. Regarding increase of K in breast tumour tissue, the increased demand for blood provision by a growing tumour supplies a base of accumulation of electrolytes like K [31]. According to Garg et al. [32] possibly during malignancy, this element may be accumulated as per requirement causing enhancement. The same role is associated with P enhancement in cancerous breast tissue. The enhanced presence of Ca might be due to crystallized calcium deposits common on breast tumours [6].

Fig. 11 displays the bar chart comparing the mean elemental concentration (± standard deviation) for 30 pairs of normal and tumour colon tissue.

The obtained results showed a very significant increase of P and S ($p < 0.001$), in the tumour tissue samples and a significant increase of K and Fe ($p < 0.05$) for the same tissues. The literature on elemental composition of colon tumour tissue is scarce, however, Benninghoff

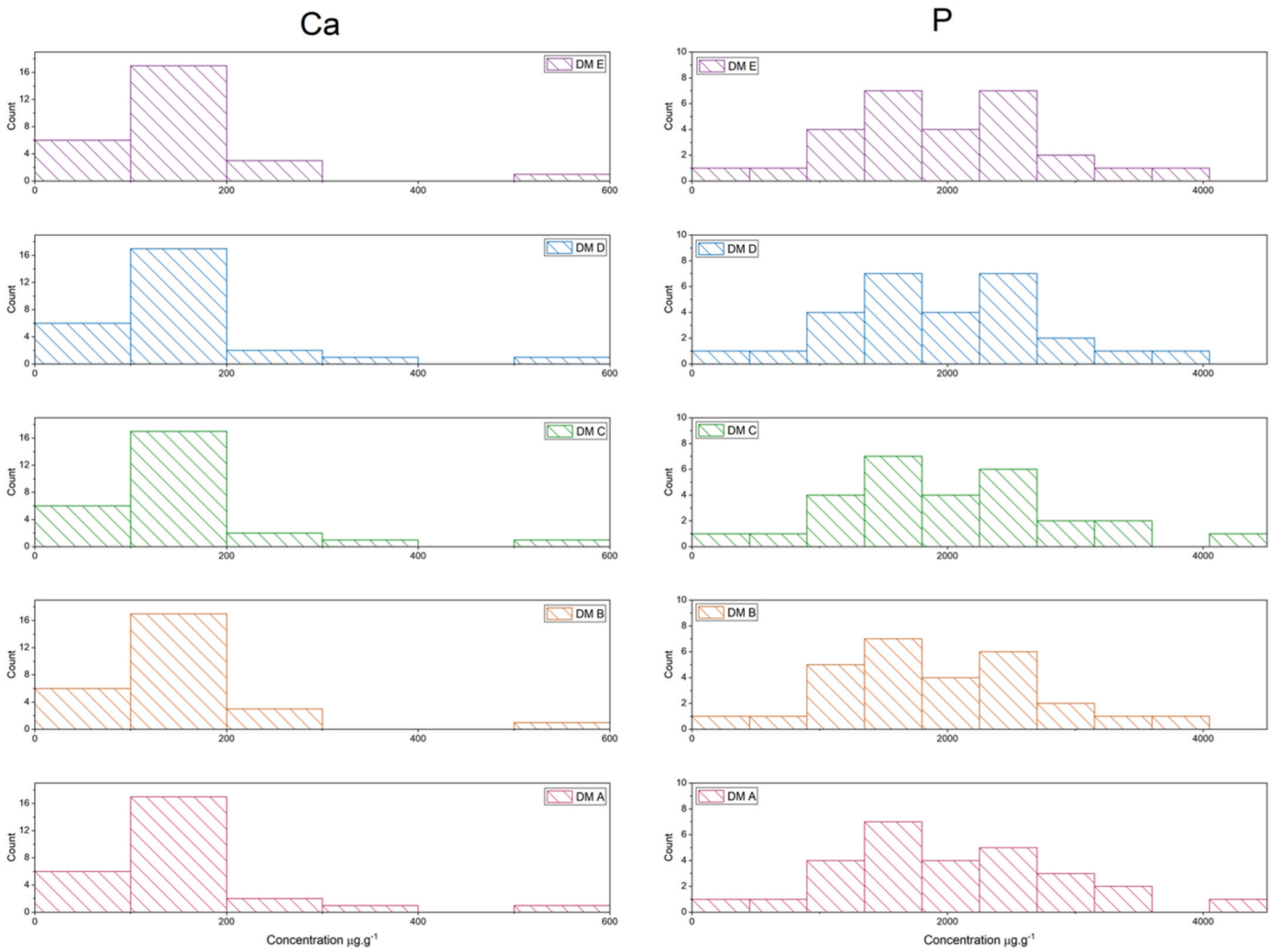

Fig. 6. Comparison of the histograms of the quantitative determinations of Ca and P using the five Dark Matrix compositions (DM_a to DM_E) for breast samples.

Table 2
Mean variation (%) of the quantitative determination to the mean value considering the five dark matrices for FFPE breast tissue for elements: P, S, K, Ca, Fe, Ni, Cu and Zn. The chosen dark matrix, with overall lower bias is highlighted.

	Δ DM_A	Δ DM_B	Δ DM_C	Δ DM_D	Δ DM_E
P	3%	3%	**1%**	2%	1%
S	3%	2%	**1%**	2%	1%
K	2%	2%	**1%**	0%	1%
Ca	2%	2%	**1%**	0%	1%
Fe	1%	0%	**1%**	2%	3%
Ni	2%	2%	**1%**	0%	1%
Cu	1%	0%	**1%**	2%	2%
Zn	1%	0%	**1%**	2%	2%

et al. [42] also determined an increase and high correlation of P, K and S in malignant tumour tissue when compared to normal colon tissue. Similarly, an increase for P, S, K was determined by Magalhães et al. [8, 9,31] and in the comparison of normal and tumour colon tissue using TXRF and EDXRF with triaxial geometry system. Conversely, an increase of Cu was determined in the tumour tissues using the same samples that was not verified in our samples. On the other hand, Majewska et al. [36] did not determine significant changes in the Cu content between benign and malignant colon tissue samples. The main difference between the elemental compositions and comparison in colon and breast samples is the behaviour for Ca and Zn, increasing in tumour breast samples but

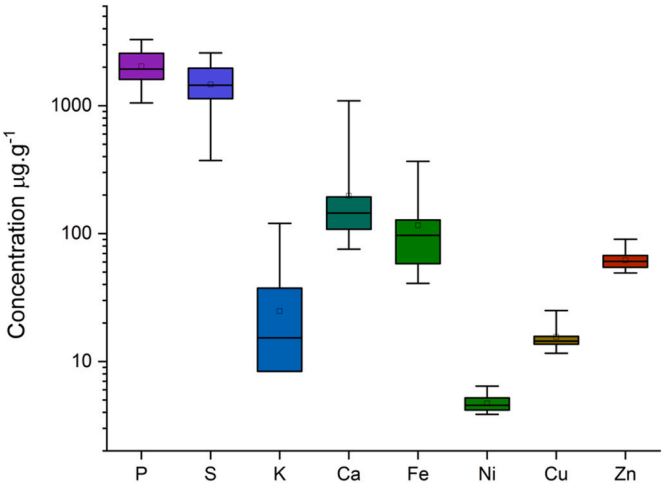

Fig. 7. - Boxplots of the elemental content of normal breast tissues using DM _C.

unaltered in colon tissue. Regarding Zn, an important element to evaluate considering its role in cell turnover and repair systems [43], no significant differences were found. In what concerns calcium, this behaviour is consistent with the scarcity of crystallized calcium deposits

Table 3
Quantitative determinations for breast tissue (without paraffin embedding) found in literature using EDXRF, TXRF, PIXE and NAA.

	P	S	K	Ca	Fe	Ni	Cu	Zn		
Breast		295 ± 120	17 ± 8 to 112 ± 12	153 ± 53 to 970 ± 90	5 ± 2 to 32 ± 3	2 ± 1	2 ± 1 to 35 ± 5	6 ± 3 to 31 ± 3	TXRF and EDXRF	[8]
				97.0 to 1830	2.4 to 36.5		0.2 to 1.8	1.0 to 8.6	TXRF	[5]
	1000 to 8240		100 to 3100		20 to 552		0.76 to 97	10 to 144	NAA	[32]
				16 to 483	3.6 to 87.9		0.1 to 103	0.1 to 9.7	EDXRF	[33]
					13.3 ± 10.4		1.20 ± 0.84	5.43 ± 3.93	TXRF	[34]
	1000 ± 280 to 5850 ± 1390	1200 ± 2210 to 6210 ± 1060	1860 ± 290 to 4280 ± 680	1010 ± 150	100 ± 20 to 200 ± 50			28 ± 8 to 130 ± 25	PIXE	[35]
	2000 ± 700	1500 ± 600	25 ± 10	200 ± 90	130 ± 90	5 ± 2	32 ± 15	60 ± 10	Present study	
Colon	1020 ± 270 to 7730 ± 2350	2370 ± 620 to 5110 ± 850	210 ± 90 to 1830 ± 440	398 ± 40 to 1340 ± 480	51 ± 23 to 260 ± 26	2.0 ± 0.5 to 10 ± 5	5 ± 2 to 28 ± 4	33 ± 10 to 100 ± 10	TXRF	[8]
					43.1 ± 8.33	3.73 ± 1.53		9.65 ± 4.5	TXRF	[36]
	4000 ± 1000	4100 ± 700	26 ± 10	400 ± 150	200 ± 100	4 ± 1	16 ± 2	130 ± 30	Present study	

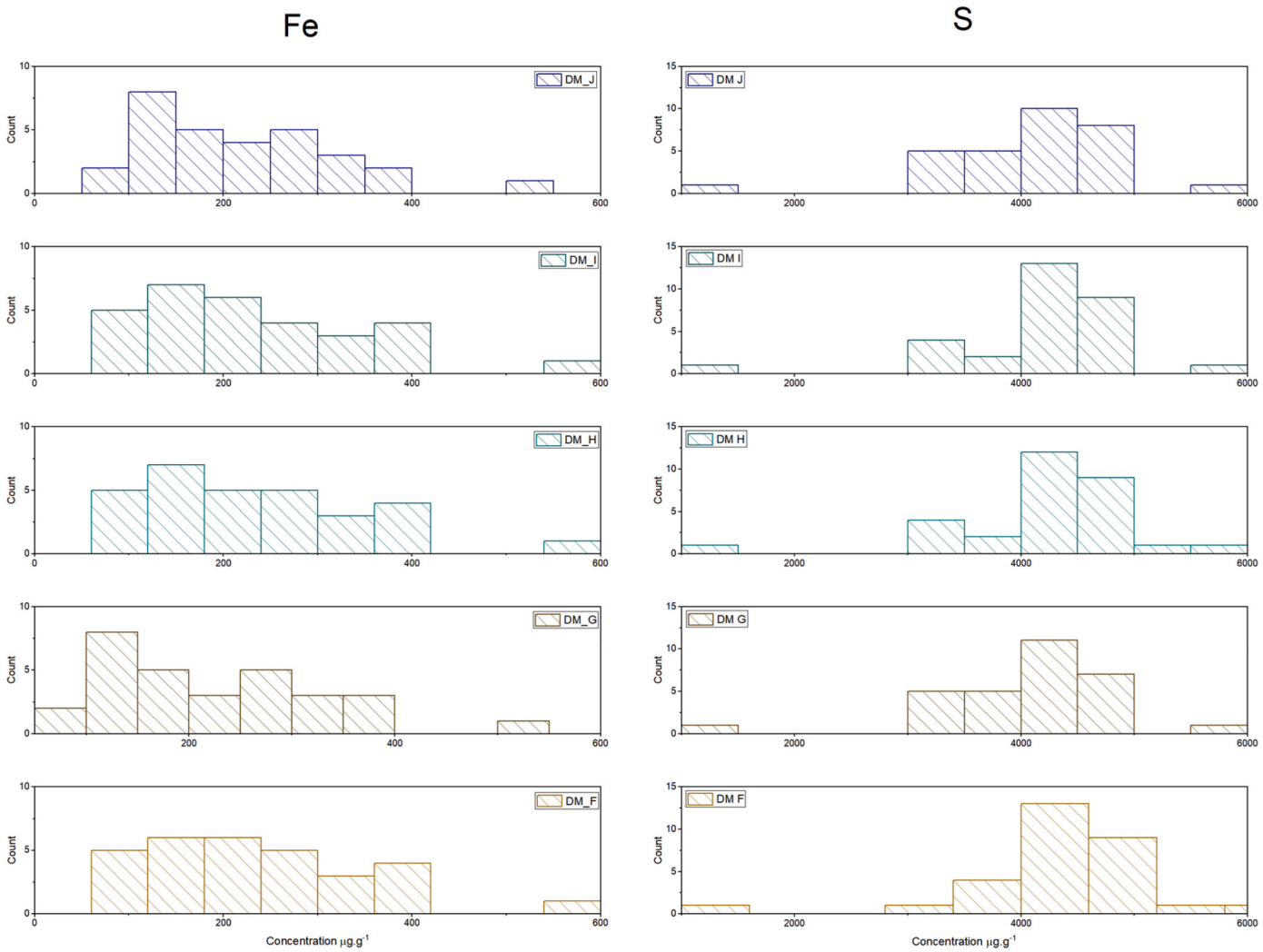

Fig. 8. Comparison of the histograms of the quantitative determinations of Fe and S using the five Dark Matrix compositions (DM_F to DM_J) for colon samples.

in colon tissues. Similar results, concerning Ca and Zn were obtained by Majewska et al. [36] and by Magalhães et al. [8] in the comparison of normal and tumour colon samples.

5. Conclusion

In this work we presented a methodology for the improvement of accuracy in the determination of the elements present in formalin-fixed paraffin-embedded (*FFPE)* human tissue samples using micro Energy Dispersive X Ray Fluorescence (micro-EDXRF) area scans, by tackling its

Table 4
Mean variation (%) of the quantitative determination for P, S, K, Ca, Fe, Ni, Cu and Zn to the mean value considering the five dark matrices for FFPE colon tissue. The chosen dark matrix, with overall lower bias is highlighted.

	Δ DM_F	Δ DM_G	Δ DM_H	Δ DM_I	Δ DM_J
P	5%	4%	3%	**1%**	3%
S	5%	4%	2%	**1%**	2%
K	5%	3%	2%	**1%**	3%
Ca	5%	3%	2%	**1%**	3%
Fe	5%	3%	2%	**1%**	3%
Ni	5%	4%	2%	**1%**	3%
Cu	5%	4%	2%	**1%**	3%
Zn	4%	4%	2%	**1%**	3%

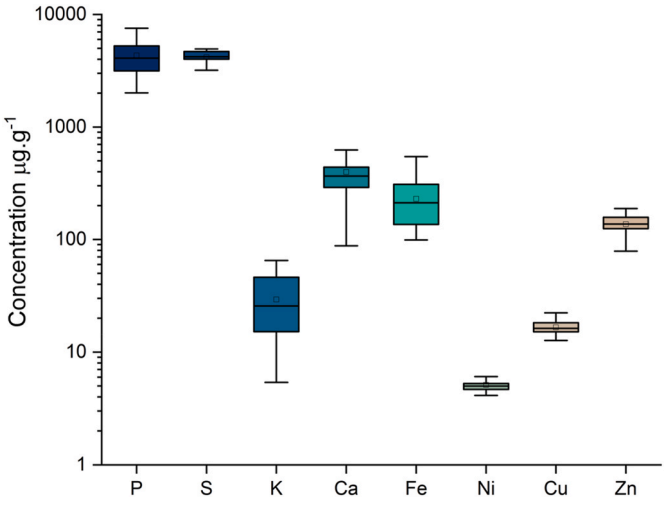

Fig. 9. Boxplots of the elemental content of normal breast tissues using DM_I.

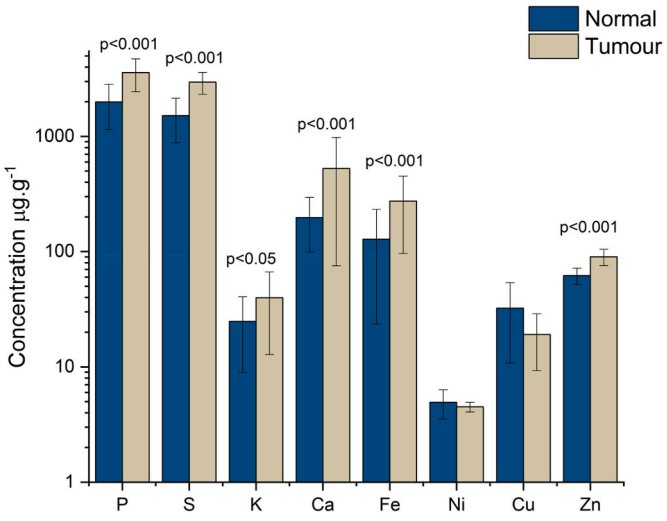

Fig. 10. Comparison of mean elemental concentration (± standard deviation) for 28 pairs of normal and tumour breast tissue. Significance in normal-tumour differences is indicated by the p-value.

major constraint – paraffin embedding.

The influence of paraffin was mitigated by developing an image treatment methodology for the retrieval of the most suitable sampling area in the FFPE block EDXRF image. Moreover, by taking advantage of the dependency of the Compton-to-Rayleigh ratio of the spectra with the mean Z of the scattering sample, the influence of paraffin in the dark matrix was overcome. This way, different matrix compositions were

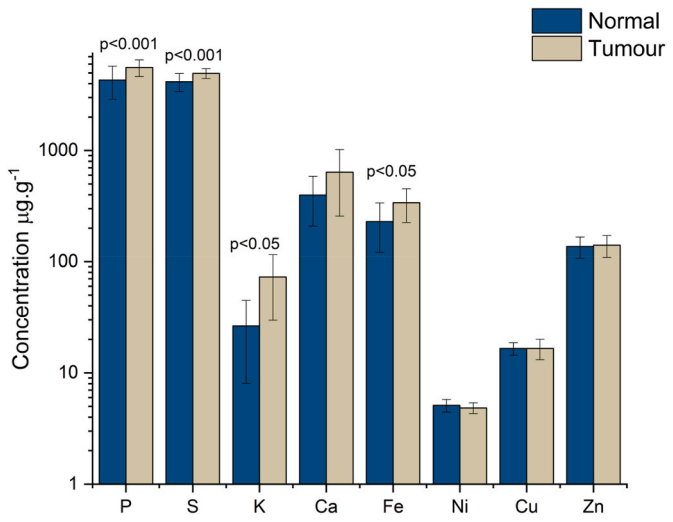

Fig. 11. Comparison of mean elemental concentration (± standard deviation) for 30 pairs of normal and tumour colon tissue. Significance in normal-tumour differences is indicated by the p-value.

found for breast and colon FFPE samples, and a similar procedure should be performed for any different tissue to be analysed in the future. It is noteworthy that the mean Z for breast is lower and presents higher uncertainty than for colon, this is most likely due to higher adipose content of the breast tissue. It is, hence, expected a much lower mean Z value for tissues such as heart or liver, when compared to colon.

By applying the developed methodology to paired normal-tumour sets of breast and colon samples, significant changes in concentration were found in elements vital for various biological and enzymatic processes. Under discussion is whether altered concentrations in tumour samples are a consequence of the disease rather than the reason for its development. This way, the accurate determination of the elemental level in neoplasm tissues and its influence on the progress of the disease is a topic of much interest.

Credit author statement

Sofia Pessanha – Conceptualization; Methodology; Writing - original draft; Writing - review & editing. Daniel Braga - Formal analysis; Ana Ensina – Formal analysis, João Silva - Formal analysis; Writing - original draft; José Vilchez – Supervision; Resources; Writing original draft, Carlos Montenegro – Resources; Writing original draft, Sofia Barbosa - Data curation; Writing original draft; Maria Luisa Carvalho - Supervision; Writing - original draft; António Dias – Conceptualization; Data curation.

Declaration of competing interest

The authors declare the following financial interests/personal relationships which may be considered as potential competing interests: Sofia Pessanha reports financial support was provided by Fundação para a Ciência e Tecnologia. Sofia Pessanha reports a relationship with Fundação para a Ciência e Tecnologia that includes: funding grants.

Data availability

Data will be made available on request.

Acknowledgments

This work was partially supported by the research centre grant UID/FIS/04559/2019 to LIBPhys-UNL from the FCT/MCTES/PIDDAC,

Portugal.

S. Pessanha acknowledges the support of FCT (Portugal) under contract CEECIND/00278/2018. Authors acknowledge Centro Hospitalar Barreiro-Montijo for allowing the current investigation and providing the samples.

References

[1] M.K. Schwartz, Role of trace elements in cancer, Cancer Res. 35 (1975) 3481–3487.
[2] M. Yaman, Comprehensive comparison of trace metal concentrations in cancerous and non-cancerous human tissues, Curr. Med. Chem. 13 (2006) 2513–2525, https://doi.org/10.2174/092986706778201620.
[3] J.J.R.F. da Silva, R.J.P. Williams, The chemical elements in biology, in: The Biological Chemistry of the Elements: the Inorganic Chemistry of Life, second ed., Oxford University Press, 2001.
[4] M.A. Zoroddu, J. Aaseth, G. Crisponi, S. Medici, M. Peana, V.M. Nurchi, The essential metals for humans: a brief overview, J. Inorg. Biochem. 195 (2019) 120–129, https://doi.org/10.1016/j.jinorgbio.2019.03.013.
[5] M.P. Silva, A. Tomal, C.A. P, A. Ribeiro-silva, M.E. Poletti, Determination of Ca , Fe , Cu and Zn and their correlations in breast cancer and normal, X Ray Spectrom. 38 (2009) 103–111, https://doi.org/10.1002/xrs.1126.
[6] J. Machado, P.M. Carvalho, A. Félix, D. Doutel, J.P. Santos, M.L. Carvalho, S. Pessanha, Accuracy improvement in XRF analysis for the quantification of elements ranging from tenths to thousands μg g −1 in human tissues using different matrix reference materials, J Anal At Spectrom 35 (2020) 2920–2927, https://doi.org/10.1039/d0ja00307g.
[7] P.M.S. Carvalho, S. Pessanha, J. Machado, A.L.M. Silva, J. Veloso, D. Casal, D. Pais, J.P. Santos, Energy dispersive X-ray fluorescence quantitative analysis of biological samples with the external standard method, Spectrochim. Acta Part B At. Spectrosc. 174 (2020), 105991, https://doi.org/10.1016/j.sab.2020.105991.
[8] T. Magalhães, A. von Bohlen, M.L. Carvalho, M. Becker, Trace elements in human cancerous and healthy tissues from the same individual: a comparative study by TXRF and EDXRF, Spectrochim. Acta Part B At. Spectrosc. 61 (2006) 1185–1193, https://doi.org/10.1016/j.sab.2006.06.002.
[9] M.L. Carvalho, T. Magalhães, M. Becker, A. von Bohlen, Trace elements in human cancerous and healthy tissues: a comparative study by EDXRF, TXRF, synchrotron radiation and PIXE, Spectrochim. Acta Part B At. Spectrosc. 62 (2007) 1004–1011, https://doi.org/10.1016/j.sab.2007.03.030.
[10] M.E. Poletti, O.D. Gonçalves, C.A. Pérez, S.D. Magalhães, A preliminary study of the distribution of trace elements in healthy and neoplastic breast tissues with synchrotron radiation X-ray fluorescence, Radiat. Phys. Chem. 71 (2004) 975–976, https://doi.org/10.1016/j.radphyschem.2004.05.007.
[11] A. Ensina, P.M. Carvalho, J. Machado, M.L. Carvalho, D. Casal, D. Pais, J.P. Santos, A.A. Dias, S. Pessanha, Analysis of human tissues using Energy Dispersive X Ray Fluorescence – dark matrix determination for the application to cancer research, J. Trace Elem. Med. Biol. 68 (2021), 126837, https://doi.org/10.1016/j.jtemb.2021.126837.
[12] M. Mantler, N. Kawahara, How accurate are modern fundamental parameter methods? The Rigaku Journal 21 (2004) 17–25. http://www.rigaku.com/downloads/journal/online-contents.html.
[13] R. Padilla, P. Van Espen, A. Abrahantes, K. Janssens, Semiempirical approach for standardless calibration in ??-XRF spectrometry using capillary lenses, X Ray Spectrom. 34 (2005) 19–27, https://doi.org/10.1002/xrs.781.
[14] B.Z.R. Sitko, Quantification in X-ray fluorescence spectrometry, X-ray spectroscopy, in: S.K. Sharma (Ed.), X Ray Spectroscopy, InTech Open, 2012, pp. 137–162.
[15] A. Banas, W.M. Kwiatek, K. Banas, M. Gajda, B. Pawlicki, T. Cichocki, Correlation of concentrations of selected trace elements with Gleason grade of prostate tissues, J. Biol. Inorg Chem. 15 (2010) 1147–1155, https://doi.org/10.1007/s00775-010-0675-5.
[16] W.M. Kwiatek, A. Banaś, M. Gajda, M. Gałka, B. Pawlicki, G. Falkenberg, T. Cichocki, Cancerous tissues analyzed by SRIXE, J. Alloys Compd. 401 (2005) 173–177, https://doi.org/10.1016/j.jallcom.2005.02.070.
[17] K. Geraki, M.J. Farquharson, M.J. Farquharson, C. Theodorakou, M. J. Farquharson, Concentrations of Fe , Cu and Zn in breast tissue : a synchrotron XRF study, Phys. Med. Biol. 47 (2002) 2327–2339.
[18] M.J. Farquharson, K. Geraki, The use of combined trace element XRF and EDXRD data as a histopathology tool using a multivariate analysis approach in characterizing breast tissue, X Ray Spectrom. 33 (2004) 240–245, https://doi.org/10.1002/xrs.684.
[19] S. Nicolás-Párraga, M. Torres, L. Alemany, A. Félix, E. Cruz, S. de Sanjosé, F. X. Bosch, I.G. Bravo, Human DNA decays faster with time than viral dsDNA: an analysis on HPV16 using pathology archive samples spanning 85 years, Virol. J. 18 (2021), https://doi.org/10.1186/s12985-021-01529-9.
[20] G.E. Falchini, A. Malezan, M.E. Poletti, E. Soria, M. Pasqualini, R.D. Perez, Analysis of phosphorous content in cancer tissue by synchrotron micro-XRF, Radiat. Phys. Chem. 179 (2021), 109157, https://doi.org/10.1016/j.radphyschem.2020.109157.
[21] A. Al-Ebraheem, K. Geraki, R. Leek, A.L. Harris, M.J. Farquharson, The use of biometal concentrations correlated with clinical prognostic factors to assess human breast tissues, X Ray Spectrom. 42 (2013) 330–336, https://doi.org/10.1002/xrs.2463.
[22] A.G. Sarafanov, T.I. Todorov, A. Kajdacsy-Balla, M.A. Gray, V. Macias, J. A. Centeno, Analysis of iron, zinc, selenium and cadmium in paraffin-embedded prostate tissue specimens using inductively coupled plasma mass-spectrometry, J. Trace Elem. Med. Biol. 22 (2008) 305–314, https://doi.org/10.1016/j.jtemb.2008.03.010.
[23] P.M. Wróbel, Ł. Chmura, P. Kasprzyk, K. Kozlowski, K. Wątor, M. Szczerbowska-Boruchowska, Feasibility study of elemental analysis of large population of formalin fixed paraffin embedded tissue samples – preliminary results, Spectrochim. Acta Part B At. Spectrosc. 173 (2020), 105971, https://doi.org/10.1016/j.sab.2020.105971.
[24] S. Pessanha, S. Silva, L.S. Martins, J.P. Santos, J.M. Silveira, Suitability of Compton-to-Rayleigh ratio in X ray Fluorescence spectroscopy: hydroxyapatite-based materials characterization, J Anal At Spectrom 35 (2020) 2920–2927, https://doi.org/10.1039/C8JA00370J.
[25] R Core Team. R: A Language and Environment for Statistical Computing, R Foundation for Statistical Computing, 2021. Url:.
[26] J. Sherman, The theoretical derivation of fluorescent X-ray intensities from mixtures, Spectrochim. Acta 7 (1955) 283–306, https://doi.org/10.1016/0371-1951(55)80041-0.
[27] S. Pessanha, S. Coutinho, M.L. Carvalho, J.M. Silveira, A. Mata, Determination of demineralization depth in tooth enamel exposed to abusive use of whitening gel using micro-Energy Dispersive X ray Fluorescence, Spectrochim. Acta Part B At. Spectrosc. 138 (2017) 8–13, https://doi.org/10.1016/j.sab.2017.10.001.
[28] S. Pessanha, C. Fonseca, J.P. Santos, M.L. Carvalho, A.A. Dias, Comparison of standard-based and standardless methods of quantification used in X-ray fluorescence analysis: application to the exoskeleton of clams, X Ray Spectrom. 47 (2018) 108–115, https://doi.org/10.1002/xrs.2819.
[29] S. Pessanha, M. Costa, M.I. Oliveira, M.E.M. Jorge, M.L. Carvalho, Nondestructive analysis of Portuguese “dinheiros” using XRF: overcoming patina constraints, Appl. Phys. Mater. Sci. Process 119 (2015) 1173–1178, https://doi.org/10.1007/s00339-015-9087-2.
[30] V.D. Hodoroaba, V. Rackwitz, Gaining improved chemical composition by exploitation of compton-to-Rayleigh intensity ratio in XRF analysis, Anal. Chem. 86 (2014) 6858–6864, https://doi.org/10.1021/ac5000619.
[31] T. Magalhães, M.L. Carvalho, A. von Bohlen, M. Becker, Study on trace elements behaviour in cancerous and healthy tissues of colon, breast and stomach: total reflection X-ray fluorescence applications, Spectrochim. Acta Part B At. Spectrosc. 65 (2010) 493–498, https://doi.org/10.1016/j.sab.2010.04.001.
[32] A.N. Garg, V. Singh, R.G. Weginwar, V.N. Sagdeo, An elemental correlation study in cancerous and normal breast tissue with successive clinical stages by neutron activation analysis, Biol. Trace Elem. Res. 46 (1994) 185–202, https://doi.org/10.1007/BF02789296.
[33] M.P. Silva, D.F. Soave, A. Ribeiro-silva, M.E. Poletti, Trace elements as tumor biomarkers and prognostic factors in breast cancer: a study through energy dispersive x-ray fluorescence, BMC Res. Notes 5 (2012) 194–205.
[34] A. Kubala, D. Banaś, J. Braziewicz, S. Góźdź, U. Majewska, M. Pajek, Analysis of elemental concentration censored distributions in breast malignant and breast benign neoplasm tissues, Spectrochim. Acta Part B At. Spectrosc. 62 (2007) 695–701, https://doi.org/10.1016/j.sab.2007.03.004.
[35] R. Hollands, N.M. Spyrou, Elemental composition changes between breast tissue with and without silicone gel sheeting and hypertrophic scar tissue, Biol. Trace Elem. Res. 71–72 (1999) 575–583, https://doi.org/10.1007/BF02784246.
[36] U. Majewska, D. Banaś, J. Braziewicz, S. Góźdź, A. Kubala-Kukuś, M. Kucharzewski, Trace element concentration distributions in breast, lung and colon tissues, Phys. Med. Biol. 52 (2007) 3895–3911, https://doi.org/10.1088/0031-9155/52/13/016.
[37] M. Piacenti da Silva, O.L.A.D. Zucchi, A. Ribeiro-Silva, M.E. Poletti, Discriminant analysis of trace elements in normal, benign and malignant breast tissues measured by total reflection X-ray fluorescence, Spectrochim. Acta Part B At. Spectrosc. 64 (2009) 587–592, https://doi.org/10.1016/j.sab.2009.05.026.
[38] S. Mirji, N.M. Badiger, K. Sanyal, S.S. Kulkarni, N.L. Misra, P.B. Gai, Determination of trace elements in normal and malignant breast tissues of different age group using total reflection X-ray fluorescence spectrometer, X Ray Spectrom. 47 (2018) 432–440, https://doi.org/10.1002/xrs.2968.
[39] O. Marques, B.M. da Silva, G. Porto, C. Lopes, Iron homeostasis in breast cancer, Cancer Lett. 347 (2014) 1–14, https://doi.org/10.1016/j.canlet.2014.01.029.
[40] B.J. Grattan, H.C. Freake, Zinc and cancer: implications for LIV-1 in breast cancer, Nutrients 4 (2012) 648–675, https://doi.org/10.3390/nu4070648.
[41] A. Dutta, M. Schaller, A.T. Franco, K. Sankavaram, B.J. Grattan, H.C. Freake, Zinc retention differs between primary and transformed cells in response to zinc deprivation, JNB (J. Nutr. Biochem.) 21 (2010) 162–170, https://doi.org/10.1016/j.jnutbio.2008.12.008.
[42] L. Benninghoff, D. von Czarnowski, E. Denkhaus, K. Lemke, Analysis of human tissues by total reflection X-ray fluorescence. Application of chemometrics for diagnostic cancer recognition, Spectrochim. Acta Part B At. Spectrosc. 52 (1997) 1039–1046, https://doi.org/10.1016/S0584-8547(96)01626-6.
[43] G.E. Gîlcă-Blanariu, S. Diaconescu, M. Ciocoiu, G. Tefănescu, New insights into the role of trace elements in IBD, BioMed Res. Int. 2018 (2018), https://doi.org/10.1155/2018/1813047.